Available online at www.sciencedirect.com
ScienceDirect
Bioorganic & Medicinal Chemistry 16 (2008) 3076–3083
Bioorganic & Medicinal Chemistry

Synthesis and antiviral activities of novel chiral cyanoacrylate derivatives with (*E*) configuration

Zhuo Chen, Xianyou Wang, Baoan Song,* Hua Wang, Pinaki S. Bhadury, Kai Yan, Huiping Zhang, Song Yang, Linhong Jin, Deyu Hu, Wei Xue, Song Zeng and Jun Wang

Center for Research and Development of Fine Chemicals, Key Laboratory of Green Pesticide and Agricultural Bioengineering, Ministry of Education, Guizhou University, Guiyang 550025, PR China

Received 24 November 2007; revised 14 December 2007; accepted 15 December 2007
Available online 21 February 2008

Abstract—The intermediate 3 is converted by the nucleophilic attack of the appropriate aryl (heterocyclic) amine under microwave irradiation into the chiral (E) isomers of title compound **4**. These compounds exhibited weak to good anti-TMV bioactivity with (*R*)-4p showing significant enhancement of disease resistance in tobacco leaves.

1. Introduction

Synthetic studies on cyanoacrylate derivatives have recently received wide attention due to their herbicidal action caused by disrupting photosynthetic electron transport.[1–3] Among them, (*Z*)-ethoxyethyl 2-cyano-3-(4-chlorophenyl)-methylamino-3-isopropylacrylate (CPNPE) has served as a model compound due to its excellent herbicidal activity.[4] In our previous work, we designed and synthesized some chiral cyanoacrylates with antiviral activity by replacing methylthio moiety with (*R*)- or (*S*)-1-phenylethylamine groups in some 2-cyano-3-methylthio-3-substituted-phenylaminoacrylates. The crystal structure of the chiral product was determined by X-ray single-crystal structure analysis which confirmed the presence of an (*E*) configuration. The bioassay showed that the chiral compound with 4-nitrophenyl moiety had no herbicidal activities in vivo, but possessed good antiviral activity.[5] Viruses are unique in the deceptive simplicity of their structure. However, this simplicity leads to a greater dependence on the host and a highly intricate relationship exists between the two which complicates the strategic designs to control plant viruses and the losses caused by them.[6] Control programs depend on our understanding of the virus–host relationship, and several conventional strategies to control virus infection have been explored but without much success. In most of the modern approaches involving antiviral action, the induced resistance is very promising to a particular strain or group of viruses. PAL, the key enzyme in the phenylpropanoid pathway, which is associated with PR gene, is strongly induced after the infection of tobacco plants with viral pathogens.[7] In order to extend our research work of cyanoacrylate as antiviral agent, we designed and synthesized some novel chiral cyanoacrylates with (*E*) configuration in which the phenylamino group was replaced by 2-nitrophenylamino, 3-nitrophenylamino, 2,4-dinitrophenylamino, 4-methylbenzothiazol-2-amino, and benzylamino groups. The synthetic route is shown in Scheme 1. The structures of **4a**–**r** were established by well-defined IR, NMR, and elemental analysis. In the bioassay conducted by half-leaf method, these new chiral compounds were found to possess weak to good anti-TMV activities. Our previous and present studies have shown the effectiveness of chiral cyanoacrylates in protecting tobacco plant against disease caused by TMV. Their mode of action and cellular targets are however still unknown. The objective of our study is to establish the role of (*R*)-4p in inducing disease resistance in tobacco leaves against virus pathogen attack, and to study the activity of enzymes or metabolites that might be involved for resistance devel-

Abbreviations: TMV, tobacco mosaic virus; CMV, cucumber mosaic virus; PAL, L-phenylalanine ammonia-lyase; SOD, superoxide dismutase; POD, peroxidase; SAR, systemic acquired resistance; PR, pathogenesis related proteins; PCR, polymerase chain reaction; BLAST, basic local alignment search tool.

Keywords: 2-Cyanoacrylates; (*E*) Configuration; Synthesis; Antiviral bioactivity; Mechanism of action.

* Corresponding author. Tel.: +86 851 362 0521; fax: +86 851 362 2211; e-mail: songbaoan22@yahoo.com

0968-0896/$ - see front matter © 2007 Elsevier Ltd. All rights reserved.
doi:10.1016/j.bmc.2007.12.035

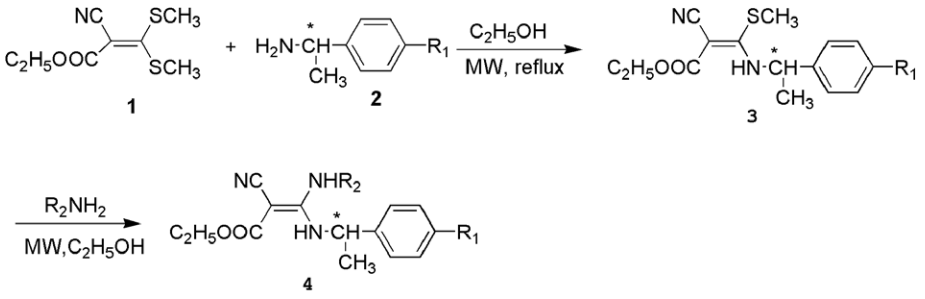

R_1 : F, Br, H; R2 = benzylamino; 2-nitrophenylamino; 3-nitrophenylamino; 2, 4-dinitrophenylamino; 4-trifluoromethylphenylamino; 6-nitrobenzothiazol-2-amino; 4-methylbenzothiazole-2-amino.

Scheme 1. Synthesis of novel chiral cyanoacrylate derivatives with (*E*) configuration.

opment. To the best of our knowledge, this is the first report on the synthesis, antiviral activity of (*E*)-ethyl 3-[(*R*) or (*S*)-1-phenylethylamino]-3-(substituted phenylamino)-2-cyanoacrylate derivatives, and the relationship between the bioactivity of (*R*)-4p and the activity of PAL, POD, and SOD enzymes and PR gene expression in tobacco. Our studies suggest that (*R*)-4p possesses antiviral activity by up-regulation of PR-1a and PR-5 gene and enhancing activity of some defensive enzyme in defense response.

2. Chemistry

2.1. Synthesis of novel chiral cyanoacrylate derivatives

Nucleophilic Michael attack by the amine at the olefinic double bond followed by the expulsion of the leaving group SCH_3 from the conjugated system seems to generate compounds **3** and **4**. To optimize the reaction conditions, the synthesis of chiral compound (*R*)-4p was carried out under several conditions. The effects of different solvents, reaction time, and the merit of using microwave irradiation over classical reaction conditions were investigated, and the results are shown in Table 1. It revealed that the presence of microwave irradiation could accelerate the reaction (entries 1–5). When the reaction time was prolonged from 5 to 20 min under microwave irradiation in refluxing ethanol at 78 °C, the yield of target chiral compound was increased from 39.4% to 52.5% (Table 1, entries 1–4). In classical method without microwave irradiation, the reaction was relatively slow and when refluxed in ethanol for 300, 600, 900, and 1200 min, 41.9%, 47.0%, 52.0%, and 53.8% yields were obtained, respectively (Table 1, entries 6–9). The reaction under microwave irradiation gave comparable yield with significant reduction of reaction time from 900 min to just 20 min, the average time ratio for the two methods being 1:30 for similar yield.

The structures of all the compounds were confirmed by ^{1}H NMR, ^{13}C NMR, elemental analysis, IR, and mass spectrometry. IR spectra of compound **4** show absorption band in the region 3220–3379 cm^{-1}, indicating the presence of NH. The characteristic C=O stretching and strong C=C vibrations appeared in the region 1639–1672 and 1539–1548 cm^{-1}, respectively. A set of peaks near 2193–2212 cm^{-1} and 1113–1165(s) were assigned to C=N and C–F vibrations, respectively. In ^{1}H NMR data, all phenyl protons showed a multiplet at δ 6.94–7.55. The chemical shifts of CH_2 ester generally appeared as a quartet in the region 4.22–4.37 ppm. The NH proton of 3 appeared downfield as a broad singlet around 9.02–11.12 ppm due to the existence of H-bond interaction between ester carbonyl and NH of phenylamino group. As for the ^{13}C NMR data of 4, all the carbon atoms were identified and the number of protons calculated from the integration curve (in ^{1}H NMR) was consistent with the molecular formula.

2.2. Crystal structure analysis

It could be seen from the X-ray single crystal analysis that chiral compound (*R*)-4b maintains a planar structure. The configuration of target compound (*R*)-4b was established as *(E)* by X-ray diffraction. The bond length of C(4)–C(6) (1.418 Å) is longer than normal C=C (1.34 Å), C(3)–O(2) (1.361 Å) is shorter than normal single C–O (1.44 Å), C(3)–C(4) (1.436 Å) and C(4)–C(5) (1.413 Å) are shorter than normal C–C (1.54 Å), C(6)–N(2) (1.341 Å) and C(6)–N(3) (1.362 Å) bonds are shorter than the normal C–N single bond (1.49 Å), suggesting the existence of an electron density delocalization among N(3)–C(6)–C(4)–C(3)–O(1), C(5), and N(2). As shown in the packing diagram of the title compound (Figs. 1 and 2), there is an intramolecular hydrogen bond interaction within N(2)–H(2)···O(1), in which N(2)–H(2) = 0.86 Å, H(2)···O(1) = 2.04, N(2)···O(1) = 2.692(3) Å, N(2)–H(2)···O(1) = 132.1° ($-x, -y + 1/2, -z + 1/2$). The N–H···O type intramolecular interaction leading to a six-membered stable cyclic structure perhaps plays a major role in stabilizing the molecules in the unit cell.

3. Antiviral activity

3.1. Preliminary antiviral activity assay

The results of bioassay in vivo against TMV are provided in Table 2. Ningnanmycin was used as reference antiviral agent. The results indicated that, the antiviral

Table 1. Results at different reaction times for the synthesis of (*E*)-ethyl-3-[(*R*)-1-(4-fluoro phenylethylamino)]-3-benzylamine-2-cyanoacrylate [(*R*)-4p]

Entry	Power (w)	Temperature (°C)	Time (min)	Solvent	Amount of the solvent (ml)	Yield[c] (%)
1[a]	50	78	5	Ethanol	10	39.4
2[a]	50	78	10	Ethanol	10	44.2
3[a]	50	78	15	Ethanol	10	49.5
4[a]	50	78	20	Ethanol	10	52.5
5[a]	50	78	30	Ethanol	10	53.1
6[b]	—	78	5 × 60	Ethanol	10	41.9
7[b]	—	78	10 × 60	Ethanol	10	47.0
8[b]	—	78	15 × 60	Ethanol	10	52.0
9[b]	—	78	20 × 60	Ethanol	10	53.8

[a] The reaction was conducted in 10 ml solvent under microwave irradiation, power 50 W.
[b] The reaction was conducted at 78 °C in 10 ml solvent under stirring without microwave.
[c] Isolated yields.

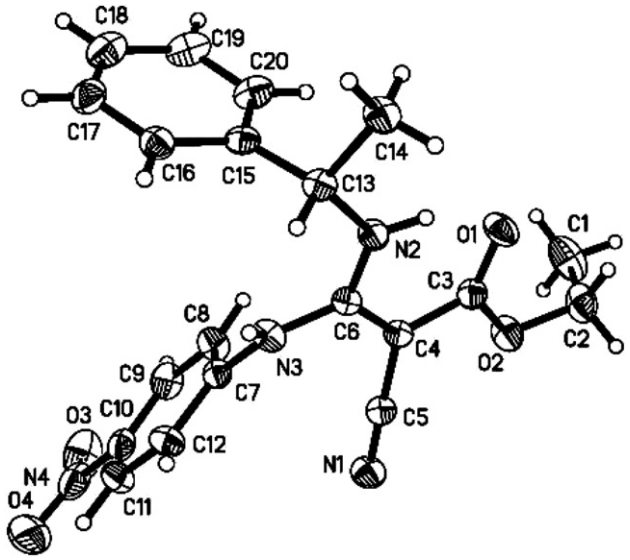

Figure 1. The molecular structure of compound (*R*)-4b.

activity is greatly dependent upon the nature of substituents. When R_1 was fluoro and R_2 was benzyl, the title compound (*R*)-4p showed higher curative rate (64.0%) than that of the reference (57.8%) and comparable inactivation rate (49.5%) with the standard Ningnanmycin (50.0%) against TMV at 500 μg/ml. It should be noted that no protection effect was observed on (*R*)-4p. The other compounds have a relatively lower antiviral activity than that of (*R*)-4p.

3.2. Effect of (*R*)-4p treatment on PAL, POD, and SOD activity in tobacco

As shown in Figure 3A, PAL levels in (*R*)-4p-treated tobacco rapidly increased by the end of the first day after the inoculation and reached 5.88 EU/mg protein on the 7th day, 37.93 times more as on the first day ($^*P < 0.05$) after inoculation. In contrast, in control and TMV, no significant increase in PAL activity was measured (Fig. 3). The PAL activity in tobacco (control and TMV) increased marginally and reached a peak at the end of the fifth day after inoculation before starting to fall gradually thereafter.

As shown in Figure 3B, it could be found that SOD activity in (*R*)-4p-treated tobacco gradually decreased from 1st day to the start of the 3rd day and then started to increase by the end of the 3rd day after inoculation. Similar trend in the change of SOD activity was observed with water-treated tobacco and not much difference was noticed within and among groups. It was found that the SOD activity in TMV gradually increased after the first day of inoculation, but the level was lower than that in water-treated by the first day ($^*P < 0.05$).

As shown in Figure 3C, it could be seen that POD activity of (*R*)-4p increased and reached a peak on the 5th day after the inoculation, then gradually decreased (Fig. 3). POD contents in (*R*)-4p-treated tobacco leaf were 8.42 times as large as that ($^*P < 0.05$) in water-treated tobacco leaf on the 1st day of inoculation. The POD activity of water and TMV treatments both reached their peaks on the 3rd and 1st day after the inoculation, but the peak value of POD activity corresponding to the control was lower than that of (*R*)-4p-treated one.

3.3. Gene expression analysis of PR-1a and PR-5 in (*R*)-4p-treated tobacco leaf

The results of product of PCR in PR-1a and PR-5 and its sequence identification, see Supporting information. In vitro synthesized single-stranded cDNA from RNA samples was isolated from leaf in water-treated tobacco and the TMV-treated tobacco and the (*R*)-4p- and TMV-treated tobacco. The differential expression analysis of the PR-1a and PR-5 gene was determined by the semi-quantitative PCR and the relative quantification real-time PCR analysis. The mRNAs of PR-1a and PR-5 gene accumulated to detectable levels in (*R*)-4p- and TMV-treated tobacco leaf, while no-detectable levels were reached in water-treated tobacco and the TMV-treated tobacco. The mRNA content of (*R*)-4p-treated tobacco leaf for PR-1a gene started to increase after 12 h and reached a peak at the end of the 2nd day before falling to the normal level. In contrast, in TMV-treated tobacco leaf, no significant increase in the levels of gene expression was noticed (Figs. 4A and 5A). The expression levels of PR-5 gene in (*R*)-4p-treated tobacco rapidly increased and reached a peak within 12 h after the inoculation and then started to decrease gradually. As

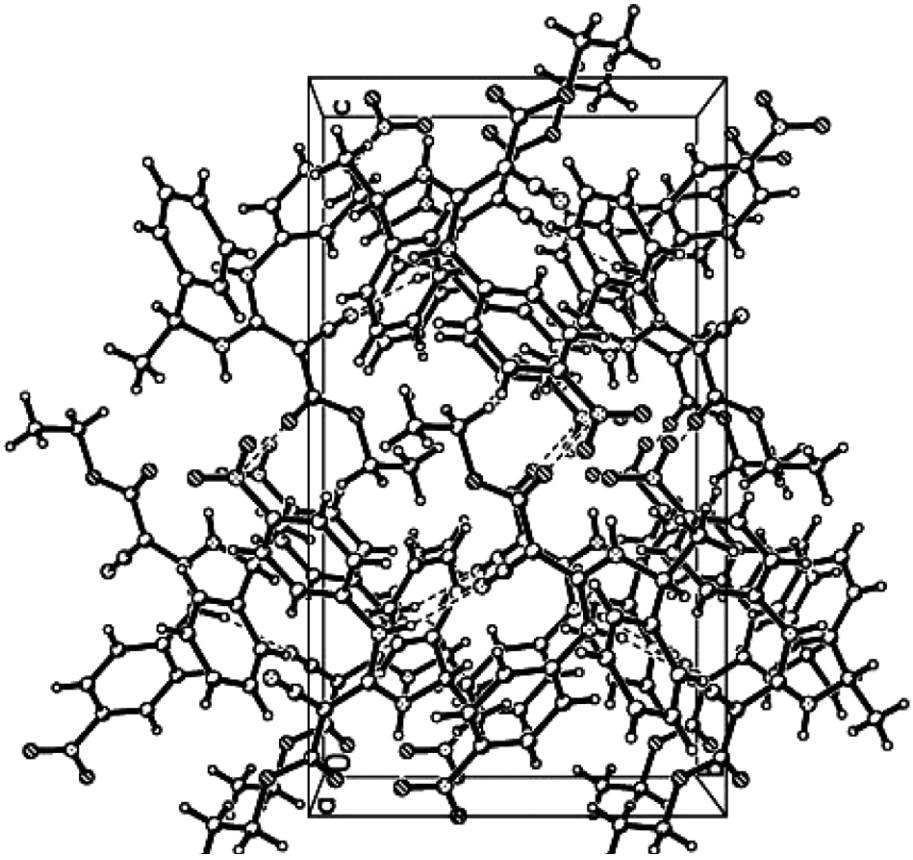

Figure 2. Packing diagram of the unit cell of compound (R)-4b.

Table 2. The protection, inactivation, and curative effect of the chiral new compounds to TMV in vivo

Agents	Concentration (mg/L)	Protection effect (%)	Inactivation effect (%)	Curative effect (%)
(*S*)-4a	500	0	0	19.7
(*R*)-4b	500	38.1 ± 4*	0	0
(*S*)-4c	500	10.0 ± 4*	0	44.8 ± 4*
(*R*)-4d	500	2.7 ± 2	0	7.5 ± 4
(*S*)-4e	500	16.7 ± 4*	0	38.7 ± 8*
(*R*)-4f	500	0	0	21.7 ± 4*
(*S*)-4g	500	7.8 ± 4*	23.2 ± *	9.6 ± 2*
(*R*)-4h	500	48.1 ± 4.*	32.3 ± 7*	20.0 ± 5*
(*S*)-4i	500	11.0 ± 2*	11.0 ± 4	0
(*R*)-4j	500	51.9 ± 7*	16.8 ± 3*	12.3 ± 4*
(*S*)-4k	500	0	15.4	0
(*R*)-4l	500	3.8 ± 1	0	28.6 ± 4*
(*S*)-4m	500	17.4 ± 3*	4.2 ± 2	0
(*R*)-4n	500	5.4 ± 4.2	14.3 ± 3*	0
(*S*)-4o	500	46.4 ± 5*	46.5 ± 4*	34.5 ± 4*
(*R*)-4p	500	65.7 ± 8*	49.5 ± 5*	64.0 ± 5**
(*s*)-4q	500	22.6 ± 3*	32.6 ± 4*	55.5 ± 5**
(*R*)-4r	500	25.0 ± 4*	5.3 ± 1	36.9 ± 4*
Ningnanmycin	500	100 ± 7**	50.0 ± 4**	57.8 ± 6**

All results are expressed as means ± SD; $n = 3$ for all groups; $^{*}P < 0.05$, $^{**}P < 0.01$.

depicted in Figures 4B and 5B, (*R*)-4p-treated tobacco leaves showed significant enhancement in the levels of gene expression, almost twice as large as compared to TMV-treated tobacco leaves within 12 h after the inoculation. In contrast, in TMV-treated tobacco leaf, no significant increase in the levels of gene expression was observed Figs. 4 and 5.

4. Discussion

Although the action mechanism of anti-TMV has not yet been elucidated, some studies show that there exists requisite association between the defense enzymes of tobacco and salicylic acid-mediated signal transduction pathway regarding pathogenesis related proteins. PAL

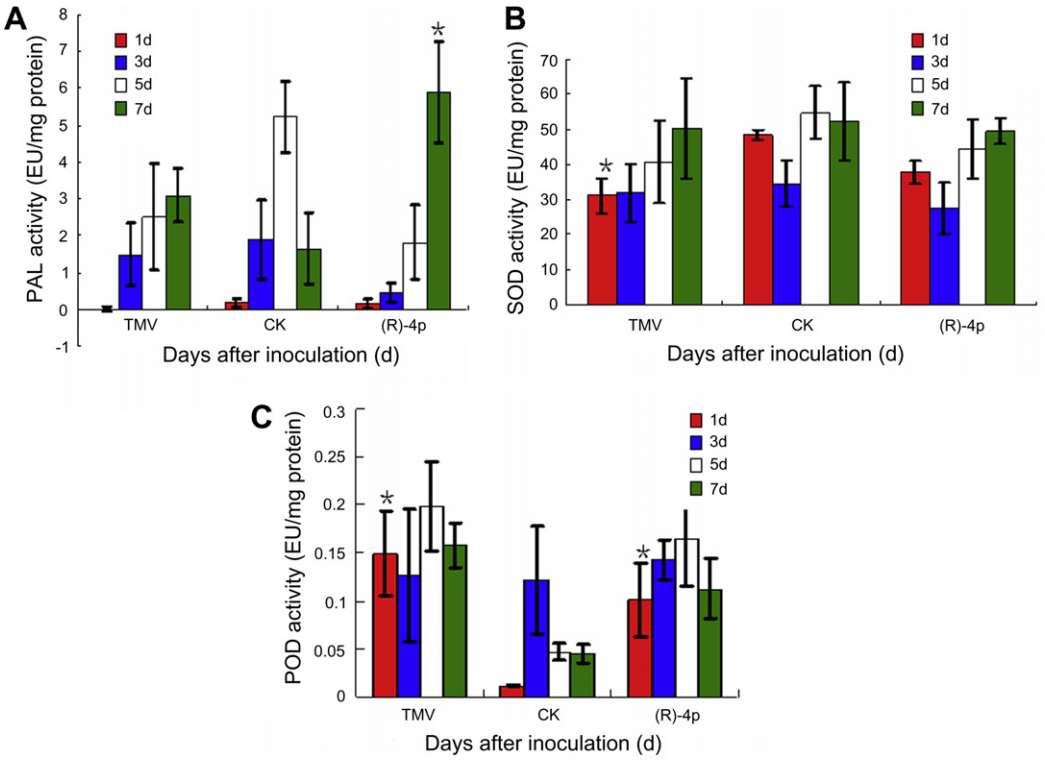

Figure 3. Effect of (*R*)-4p treatment on PAL and SOD and POD activity in *Nicotiana tabacum*. *Nicotiana tabacum* inoculated by TMV was treated with (*R*)-4p at 500 ppm for 1, 3, 5, and 7 day. Leaf sample extracts using homogenized and centrifuged methods were used to determine the PAL and SOD and POD activities as described in Section 6. Water treatment and TMV treatment were used for negative and positive controls. Data are expressed as means ± SD ($n = 3$) of three individual experiments. One-way ANOVA revealed significant difference ($^{*}P < 0.05$).

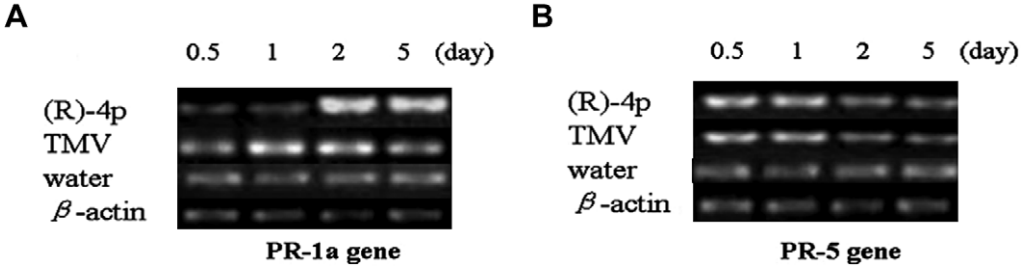

Figure 4. Semi-quantitative RT-PCR analysis of RNA isolated from tobacco leaf. The figure shows that 20 cycles were performed and the amplified products were resolved on a 1.5% agarose gel by following the RT. Parts A and B in the figures indicate result of PR-1a and PR-5 gene expression treated by (*R*)-4p compound at 500 ppm for 0.5, 1, 2, and 5 day, respectively. Lanes 1–4 represent the amount of PCR amplification at period four. β-Actin gene served as an internal reference gene.

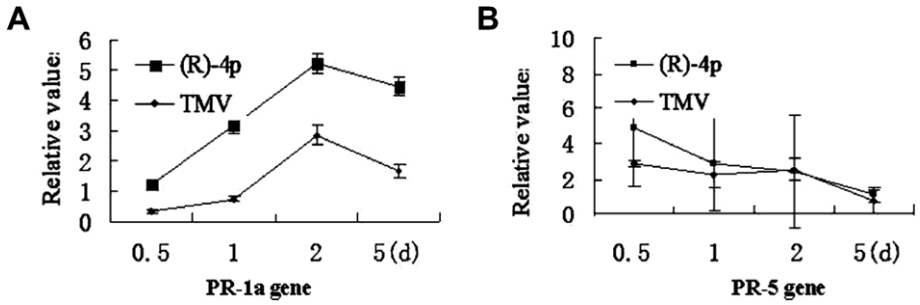

Figure 5. Real-time PCR analysis of RNA isolated from tobacco leaf. Letters A and B in the figures indicate the results of PR-1a and PR-5 gene expression ratio through C_T value formula $\Delta\Delta C_T = \Delta C_{T(test)} - \Delta C_{T(calibrator)}$. Relative values of real-time PCR between target gene and β-actin gene were calculated, each value represents the mean ± SD ($n = 4$) and each experiment was performed in triplicate sets. The data were analyzed by one-way ANOVA.

is a rate-limiting enzyme in the activation of the phenylpropanoid pathway, and an increase in PAL activity is associated with biosynthesis of active metabolites, such as salicylic acid, which is used for molecular signal in plant SAR defense pathways.[8] POD is also a very important enzyme in the plant defense reaction and is involved in the scavenging of reactive oxygen species. The increase in POD activity promotes the cross-link of lignin, strengthens the structure barrier, and enhances disease resistance.[9–12] Rasmussen has shown that SA could enhance the activity of POD and PAL.[13] PR-1a and PR-5 are regulation proteins of downstream in SA signal pathway that play a significant role in antiviral, antifungal, and wound repair.[14–16] Our studies have shown that PR-1a and PR-5 gene was induced to up-regulation by (*R*)-4p compound at 500 mg/ml on the 1st day after inoculation. Meanwhile, the activity of PAL and POD were increased from 1st day to 5th day after inoculation. These results show that there is significant association between curative effect and up-regulation of PR-1a and PR-5 gene against anti-TMV by (*R*)-4p to enhance defense enzymes activity level. Future research would be focused on studying the action mechanism between gene regulation and anti-TMV, and the knockdown technique to evaluate the antiviral effect against target gene.

5. Conclusion

In conclusion, a series of novel (*E*)-ethyl-3-[(*R*)- or (*S*)-1-phenyl-ethylamino]-3-(substituted phenylamino)-2-cyano-acrylate derivatives were synthesized by the treatment of chiral intermediate 3 with aryl (heterocyclic) amine under microwave irradiation. This method is easy, rapid, and moderate-yielding for the synthesis of title chiral compounds **4**. Their structures were verified by spectroscopic data. The results of bioassay showed that these title compounds exhibited weak to good anti-TMV bioactivity. Title compounds (*R*)-4p showed better biological activity than their structurally related analogues **4a**–**o**, **4q**–**r**. Preliminary studies showed that treatment by compound (*R*)-4p can significantly enhance disease resistance of tobacco leaf and substitute for antiviral agent control of TMV diseases in tobacco.

6. Experimental

The melting points of the products were determined on a XT-4 binocular microscope (Beijing Tech Instrument Co., China). The IR spectra were recorded on a Bruker VECTOR 22 spectrometer in KBr disk. ^{1}H and ^{13}C NMR (solvent $CDCl_3$) spectra were recorded on a JEOL-ECX 500 NMR spectrometer at room temperature using TMS as an internal standard. Elemental analysis was performed on an Elementar Vario-III CHN analyzer. Microwave reaction was performed on a Focused Microwave Synthesizer, Discover™ LabMate (with a power of 50 W), according to Huang's and Zhou's methods.[17,18] Analytical TLC was performed on silica gel GF254. Column chromatographic purification was carried out using silica gel. All reagents were of analytical reagent grade or chemically pure. All solvents were dried, deoxygenated, and redistilled before use. 2-Cyano-3,3-dimethylthioacrylate was prepared according to the literature method.[19]

6.1. General procedure for the preparation of intermediates 3a–d

A solution of ethyl 2-cyano-3,3-dimethyl thioacrylate (0.4 mmol) in EtOH (20 ml) was stirred, followed by the addition of [(*S*)-1-(4-fluorophenylethyl]amine] or [(*R*)-1-(4-fluorophenylethyl) amine] (0.4 mmol). The mixture was irradiated in the microwave oven at 78 °C and 50 W for 10 min. The solvent was removed under reduced pressure. The crude product was purified by column chromatography on a silica gel (eluent, ethyl acetate/petroleum ether, 4:1, v/v) to give the intermediates **3a**–**d**. The structure was confirmed by ^{1}H NMR, ^{13}C NMR, IR, and elemental analysis (see Supporting information).

6.2. General procedure for the preparation of title chiral compounds 4

A solution of ethyl intermediate 3 (0.72 mmol) in EtOH (10 ml) was stirred, followed by the addition of substituted phenylamine or 2-aminobenzothiazole (0.72 mmol). The resulting mixture was irradiated in the microwave at 78 °C, 60 W for 20 min. The course of the reaction was followed by TLC. The mixture was poured into ice water (100 ml), and acidified with 10% HCl to a pH of 6–7, and filtered. The residue was purified by column chromatography on silica gel (eluent, ethyl acetate/petroleum ether, 1:4, v/v) to give title compounds **4** (see Supporting information).

6.3. Crystal structure determination

In order to study the single-crystal structure (Figs. 1 and 2), X-ray intensity data were recorded on a Rigaku Rax-is-IV diffraction meter using graphite monochromatic MoKα radiation ($\lambda = 0.71073$ Å). In the range $2.14° \leqslant \theta \leqslant 25.01°$, 3741 independent reflections were obtained. Intensities were corrected for Lorentz and polarization effects and empirical absorption, and all data were corrected using SADABS program.[22] The structure was solved by direct methods SHELXS-97 program.[21] All the non-hydrogen atoms were refined on $F2$ anisotropically by full-matrix least squares method. The hydrogen atoms were located from the difference Fourier map, but their positions were not refined. The contributions of these hydrogen atoms were included in structure-factor calculations. The final least-square cycle gave $wR = 0.1307$, $R = 0.0539$ for 9478 reflections with $I > 2\sigma(I)$; the weighting scheme, $w = 1/[\sigma^2(F_o^2)+(0.0.0852P)^2 + 0.000P]$, where $P = [(F_o^2) + 2F_c^2]/3$. The max and min difference peaks and holes were 0.198 and -0.263 e A^{-3}, respectively, $s = 1.107$. Atomic scattering factors and anomalous dispersion corrections were taken from International Table for X-ray Crystallography.[20] Crystallographic data (excluding structure factors) for the structure have been deposited with the Cambridge Crystallographic Data Center as supplementary publication No. CCDC-299719.

Table 3. Sequences of gene-specific primers used in RT-PCR analysis

Gene family	Accession No.	5′ primer	3′ primer
β-Actin	U60495	5′-gacatgaaggaggagcttgc-3′	5′-atcatggatggctggaagag-3′
PR-1a	X12737	5′-caatacggcgaaaacctagctga-3′	5′-cctagcacatccaacacgaa-3′
PR-5	X03913	5′-gcttccccttttatgccttc-3′	5′-cctgggttcacgttaatgct-3′

6.4. Protection and inactivation and cure effect of compound against TMV in vivo

Purification of TMV was assessed by Gooding's method, as described in Supporting information.[23] The bioactivity assay for protection and inactivation and cure effect was assessed according to Li's method[24] (see Supporting information).

6.5. Determination of PAL and POD and SOD activity

The leaf samples were homogenized in the 2-mercaptoethanol-boric acid buffer (5 mM, pH 8.8) on the ice bath and centrifuged. The supernatant was used for experiment. PAL and POD and SOD activities were determined by He's method,[25] Polle's method,[26] and Beauchamp's method,[27] respectively (see Supporting information).

6.6. RT-PCR assay

Trizol kit was used according to the standard protocol for total RNA isolation. Prior to RT-PCR, the total RNA samples were treated with DNase I for 10 min and quantified by spectrophotometry and identified by agarose gel electrophoresis.[28] cDNA was synthesized with oligo $(dT)_{18}$ at the 3′ end of mRNA as a primer. Total RNA (1 μg) was used for template of first-strand cDNA synthesis using extend reverse transcriptase. Reverse transcription was carried out at 37 °C for 1 h. The single-stranded DNA mixture was used as template in PCR. The primers for PCR amplification are shown in Table 3. The PCR was performed in Tris–HCl buffer (10 mM, pH 8.3), KCl (50 mM), $MgCl_2$ (1.8–2.0 μl), dNTPs (0.02 μM), primers (0.04 μM), and DNA polymerase (1 U). PCR amplification steps consisted of a preliminary denaturation step at 94 °C for 1 min, followed by 35 cycles at 94 °C for 40 s, at 58 °C for 40 s, and at 72 °C for 50 s on icycle of Bio-Rad. PCR products were separated on 1.5% agarose gel in 0.5× TBE buffer and visualized under UV light after staining with ethidium bromide.[29]

6.7. Semi-quantity PCR for expression of gene

In order to assess relative expression levels of target-gene in water-treated tobacco and (*R*)-4p- and TMV-treated tobacco and tobacco by inoculated TMV only, semi-quantity PCR consisting of 20 cycles (within the logarithmic range of amplification of gene) with putting primer of β-actin serving as an internal reference gene was employed for the study. The amplified products were analyzed on a 1.5% agarose gel by the method of Mohamed.[30]

6.8. The relative quantification real-time PCR for expression of the target gene

The relative quantification real-time PCR was carried out with iCycler IQ according to manufacturer's protocol with primer of β-actin serving as an internal reference gene. Precautions were taken to ascertain reliable quantitative results: Log-linear dilution curves were performed with primers for the target gene as well as with primers for the β-actin. Reactions performed without reverse transcriptase or without template did not result in any product. By following PCR, 110 steps for melt curve analysis were completed in 10 s at temperature ranging from 40 to 95 °C. The amplification efficiency was 95–99% for PR-1a and PR-5 gene, respectively (the standard curve figure is not shown). Each target gene peak was assigned an arbitrary quantitative value correlated to the β-actin gene peak, according to the formula $\Delta\Delta C_T = \Delta C_{T(test)} - \Delta C_{T(calibrator)}$, C_T being the cycle threshold. Rates of stimulation of RNA expression were calculated from the ΔC_T values at various time points.[31]

6.9. Statistical analysis

All statistical analyses were performed with SPSS 10.0. Data were analyzed by one-way analysis of variance (ANOVA). Mean separations were performed using the least significant difference method (LSD test). Each experiment had three replicates and all experiments were run three times with similar results. Measurements from all the replicates were combined and treatment effects analyzed.

Acknowledgments

The authors thank the National Key Program for Basic Research (No. 2003CB114404), the Cultivation Fund of the Key Scientific and Technical Innovation Project, Ministry of Education of China (No.705039), and National Basic Research Priorities Program (No. 2005CCA01500), the National Natural Science Foundation of China (No.20672024) for the financial support.

Supplementary data

Supplementary data associated with this article can be found, in the online version, at doi:10.1016/j.bmc.2007.12.035.

References and notes

1. Wang, Q. M.; Li, H.; Li, Y. H. *J. Agric. Food. Chem.* **2004**, *52*, 1918.
2. Wang, Q. M.; Sun, H. K.; Cao, H. Y. *J. Agric. Food. Chem.* **2003**, *51*, 5030.
3. Huppatz, J. L. *Weed Sci.* **1996**, *44*, 743.
4. Mackay, S. P.; Omalley, P. J. *Naturforschung* **1993**, *48c*, 191.
5. Song, B. A.; Zhang, H. P.; Wang, H.; Yang, S.; Jin, L. H.; Hu, D. Y.; Pang, L. L.; He, W. *J. Agric. Food. Chem.* **2005**, *53*, 7886.
6. Hari, V.; Das, P. In *Plant disease virus control*; Hadidi, A., Khetarpal, R. K., Koganezawa, H., Eds.; APS Press: St. Paul, 1998; pp 417–427.
7. Shadle, G. L.; Wesley, S. V.; Korth, K. L.; Chen, F.; Lamb, C.; Dixon, R. A. *Phytochemistry* **2003**, *64*, 153.
8. Milosevic, N.; Slusarenko, A. *J. Mol. Plant. Pathol.* **1996**, *49*, 143.
9. Wang, Y. C.; Hu, D. W.; Zhang, Z. G.; Ma, Z. G.; Zheng, X. B.; Li, D. B. *Physiol. Mol. Plant Pathol.* **2003**, *63*, 223.
10. Sticher, L.; Mauch-Mani, B.; Métraux, J. P. *Annu. Rev. Phytopathol.* **1997**, *35*, 235.
11. Malamy, J.; Carr, J.; Klessigm, D.; Raskin, I. *Science* **1990**, *250*, 1002.
12. Hahlbrock, K.; Scheel, D. *Plant Mol. Biol.* **1989**, *40*, 347.
13. Rusmussen, J. B.; Hammersschmidt, R.; Zook, M. N. *Plant Physiol.* **1991**, *97*, 1342.
14. Van Loon, L. C. *Plant Mol. Biol.* **1985**, *4*, 111.
15. Tornero, P.; Gadea, J.; Conejero, V. *Mol. Plant Microbe Interact.* **1997**, *10*, 624.
16. Cheong, N. E.; Choi, Y. O.; Kim, W. Y.; Kim, S. C.; Cho, M. J.; Lee, S. Y. *Physiol. Plant.* **1997**, *101*, 583.
17. Huang, W.; Yang, G. F. *Bioorg. Med. Chem.* **2006**, *14*, 8280–8285.
18. Zhou, Z. Z.; Yang, G. F. *Bioorg. Med. Chem.* **2006**, *14*, 8666–8674.
19. Liu, X.; Huang, R. Q.; Cheng, M. R.; Zhao, Y. G.; Li, Z. G. *Chem. J. Chin. Univ.* **1999**, *20*, 1404.
20. Sheldrick, G. M. In *Program for Empirical Absorption Correction of Area Detector Data*; University of Gottingen: Germany, 1996.
21. Sheldrick, G. M. In *SHELXTL V5.1, Software Reference Manual*; Bruker AXS, Inc.: Wisconsin, 1997.
22. Wilson, A. J.. In *International Table for X-ray Crystallography*; Kluwer Academic Publishers: Dordrecht, 1992; Vol. C,, pp 219–222, 500–502.
23. Gooding, G. V., Jr.; Hebert, T. T. *Phytopathology* **1967**, *10*, 1285.
24. Li, S. Z.; Wang, D. M.; Jiao, S. M. In *Pesticide Experiment Methods-Fungicide Sector*; Li, S. Z., Ed.; Agriculture Press of China: Beijing, 1991; pp 93–94.
25. He, Z. P. In *A Guide to Experiments of Chemical Control for Crops*; He, Z. P., Ed.; Beijing Agricultural University Press: Beijing, 1933; pp 30–31.
26. Polle, A.; Otter, T.; Seifert, F. *Plant Physiol.* **1994**, *106*, 53.
27. Beauchamp, C.; Fridovich, J. *Anal. Biochem.* **1971**, *444*, 276.
28. Yamakawa, H.; Kamada, H.; Satoh, M.; Ohashi, Y. *Plant Physiol.* **1998**, *118*, 1213.
29. Anand, A.; Zhou, T.; Trick, H. N.; Gill, B. S.; Bockus, W. W. *J. Exp. Bot.* **2003**, *54*, 1101.
30. Faize, M.; Faize, L.; Ishitaka, M.; Ishii, H. *Physiol. Mol. Plant Pathol.* **2004**, *64*, 319.
31. Yuan, J. S.; Reed, A.; Chen, F.; Stewart, C. N. *BMC Bioinform.* **2006**, *7*, 85.